CANCER GENOMICS & PROTEOMICS *14*: 53-68 (2017)
doi:10.21873/cgp.20018

Expression Profiling of a Human Thyroid Cell Line Stably Expressing the *BRAF*^{V600E} Mutation

BYOUNG-AE KIM[1*], HYEON-GUN JEE[1*], JIN WOOK YI[1,2*], SU-JIN KIM[1,2], YOUNG JUN CHAI[3], JUNE YOUNG CHOI[4] and KYU EUN LEE[1,2]

[1]*Cancer Research Institute, Seoul National University College of Medicine, Seoul, Republic of Korea;*
[2]*Department of Surgery, Seoul National University Hospital, Seoul National University College of Medicine, Seoul, Republic of Korea;*
[3]*Department of Surgery, Seoul National University Boramae Medical Center, Seoul, Republic of Korea;*
[4]*Department of Surgery, Seoul National University Bundang Hospital, Seoul National University College of Medicine, Seongnam, Republic of Korea*

Abstract. *Background/Aim: The BRAF^{V600E} mutation acts as an initiator of cancer development in papillary thyroid carcinoma (PTC). Gene expression changes caused by the BRAF^{V600E} mutation may have an important role in thyroid cancer development. Materials and Methods: To study genomic alterations caused by the BRAF^{V600E} mutation, we made human thyroid cell lines that harbor the wild-type BRAF gene (Nthy/WT) and the V600E mutant-type BRAF gene (Nthy/V600E). Results: Flow cytometry and western blotting showed stable transfection of the BRAF gene. In functional experiments, Nthy/V600E showed increased anchorage-independent growth and invasion through Matrigel, compared to Nthy/WT. Microarray analysis revealed that 2,441 genes were up-regulated in Nthy/V600E compared to Nthy/WT. Gene ontology analysis showed that the up-regulated genes were associated with cell adhesion, migration, and the ERK and MAPK cascade, and pathway analysis showed enrichment in cancer-related pathways. Conclusion: Our Nthy/WT and Nthy/V600E cell line pair could be a suitable model to study the molecular characteristics of BRAF^{V600E} PTC.*

The *BRAF*^{V600E} mutation is a well-known driver mutation with a single nucleotide change of thymine to adenine at position 1799. This mutation results in a valine to glutamic acid substitution at amino acid 600 (c1799T>A, pV600E) and leads to carcinogenesis by activating the BRAF kinase cascade (1). The BRAF^{V600E} mutation accounts for 95% of *BRAF* gene alterations and is the most common genetic variation in papillary thyroid carcinoma (PTC) (2). The prevalence of BRAF^{V600E} mutation in PTC is 29-83% (3).

Previous studies have reported that the BRAF^{V600E} mutation correlates with advanced disease such as extrathyroidal extension or lymph node metastasis, but is not clearly linked with overall survival. To explain cancer progression according to *BRAF* mutation, secondary gene expression alterations caused by the BRAF^{V600E} mutation may play important roles (4-6).

Nthy-ori 3-1 (hereafter referred to as Nthy) is an immortalized thyroid follicular epithelial cell line derived from normal adult thyroid tissue that has been transfected with a plasmid encoding the SV40 large T gene. Nthy cells are useful for studies involving the control of growth and function of the human thyroid, since it is the only human normal thyrocyte-derived cell line (7). Using a MCSV promoter-based lentivirus system, Nthy/*BRAF* cells expressing either wild-type or mutant *BRAF* were successfully developed. Functional and genomic tests were conducted to explore the biological and genomic alterations caused by *BRAF*^{V600E} in normal thyroid cells.

Materials and Methods

BRAF expression in Nthy cells by lentivirus transduction. The full-length coding sequences of wild-type *BRAF* and *BRAF*^{V600E} were amplified by PCR from TPC1 and 8505c cells. PCR amplification products were cloned into the pCDH-MCS-T2A-copGFP-MCSV lentiviral vector (System Biosciences, Mountain View, CA, USA) and packaged by co-transfection with psPAX2 and pMD2.G plasmids with Lipofectamine 2000 (Invitrogen, Carlsbad, CA, USA) in HEK293FT (Invitrogen, Carlsbad, CA, USA) cells. Virus was harvested and concentrated by ultracentrifugation 48 h later. Titers

*These Authors contributed equally to this study.

Correspondence to: Kyu Eun Lee, Seoul National University Hospital & College of Medicine, 101 Daehak-ro, Jongno-gu, Seoul, 03080, Republic of Korea. Tel: +82 220722081, Fax: +82 27663975, e-mail: kyueunlee@snu.ac.kr

Key Words: Thyroid cancer, Nthy-ori 3-1 cell, *BRAF*^{V600E}, signal transduction, microarrays.

were determined by flow cytometry as percentage of green fluorescent protein (GFP)-positive cells. For stable cell line generation, Nthy-ori 3-1 cells were treated with different titers of lentivirus for 24 h and examined for GFP expression after 3 days. Titers that generated at least 95% GFP-positive cells were chosen for further culture. Cells with low/intermediate/high GFP expression were sorted using a FACSAria flow cytometer (BD biosciences, San Jose, CA, US), and only cells with high GFP expression survived and proliferated.

Cell morphology and DNA sequencing. Transfected cells were observed using a microscope. The cells were cultured in 60-mm dishes until confluent monolayers were reached and then detached using a cell scraper. Genomic DNA was extracted using the QIAamp DNA kit (Qiagen, Hilden, Germany) according to the manufacturer's recommendations. DNA was quantified using a Nanodrop ND-1000 spectrophotometer and used as template for PCR amplification of *BRAF* exon 15. PCR was performed using GeneAmp® PCR System 9700 (Applied Biosystems; Life Technologies, Carlsbad, CA, USA) as follows: initial denaturation at 95˚C for 1 min was followed by 35 cycles of denaturation at 95˚C for 15 sec, annealing at 58˚C for 15 sec, and extension at 72˚C for 15 sec. The PCR primer and DNA sequencing services were provided by Cosmo Genetech (Cosmo Genetech, Seoul, Korea). The primer sequences used in this study were as follows: *BRAF* exon 15: F 5'-TGAAGACCTCACAGTAAAAATAGGTG-3', *BRAF* exon 15: R 5'-TCCACAAAATGGATCCAGACA-3'.

Flow cytometry. Nthy cells infected with empty vector, vector encoding wild-type *BRAF*, or vector encoding $BRAF^{V600E}$ were fixed with FCM fixation buffer (Santa Cruz Biotechnology, Santa Cruz, CA, USA) on ice for 15 min. Fixed samples were washed in phosphate buffered saline (PBS) and permeabilized on ice for 10 min in FCM Permeabilization (Santa Cruz Biotechnology). Samples were washed and resuspended. Single cell suspensions were incubated with phycoerythrin (PE)-conjugated anti-phospho-p44/42 MAPK (Cell Signaling Technology; Beverly, MA, USA) for 1 h. The labeled cells were detected using a BD FACS Diva 8.0 System (Becton Dickinson, San Jose, CA, USA) according to the manufacturer's protocols. Gating was implemented on the basis of negative control staining profiles.

Western blotting. Cells were cultured in 100 mm dishes until confluent monolayers were reached. Cells were cultured for 24 h with 10% fetal bovine serum (FBS) or no FBS. Cells were washed twice with PBS and detached from the culture plate using a cell scraper. Cells were lysed on ice for 15 min with radio-immuno-precipitation assay (RIPA) buffer (Thermo Scientific, Rockford, IL, USA), which contains 1% proteinase inhibitors. The samples were loaded onto a 10% SDS-polyacrylamide gel and subjected to electrophoresis on ice. The proteins resolved were transferred onto polyvinylidene fluoride (PVDF) membrane for 1 h and blocked for 1 h at room temperature with 5% skim milk. The membranes were incubated overnight at 4˚C with the primary antibodies. Anti-alpha tubulin (diluted 1:1,000) was obtained from Santa Cruz Biotechnology. Anti-ERK1/2 (diluted 1:1,000) and anti-phospho-ERK1/2 (diluted 1:1,000) were obtained from Cell Signaling Technology. The membranes were washed in Tris-buffered saline-Tween 20 (TBST) and incubated with the secondary antibody.

Soft-agar assay. Nthy cells infected with empty vector, vector encoding wild-type *BRAF*, or vector encoding $BRAF^{V600E}$ were seeded at 3,000 cells per well in 24-well plates in a top layer of 0.4% agarose (Cell Biolabs) on a base layer of 0.6% agarose. Culture medium containing DMSO or $BRAF^{V600E}$ kinase inhibitors (PLX-4032, BioVision, San Francisco, CA, USA) was added to each well and cultured at 37˚C in the presence of 5% CO_2 for 7 days. The number of colonies containing more than 25 cells was counted using a microscope.

Invasion assay. The invasion assay was performed using the xCELLigence DP Real Time Cell Analyzer and CIM-16 plates with 8-μm pore membranes. The bottom electrodes of the CIM-16 plates were coated with 0.2% gelatin and incubated in a laminar air flow chamber for 30 min. The upper chambers of CIM-16 plates were coated with 20 μl of 0.5 mg/ml growth factor-reduced Matrigel (BD Bioscience, Bedford, MA, USA) prepared in FBS-free RPMI medium. Matrigel was allowed to equilibrate for 2 h at 37˚C in 5% CO_2. RPMI medium with 10% FBS was added to the bottom chambers. Empty vector control cells (Nthy/Vector), wild-type *BRAF* cells (Nthy/WT), or $BRAF^{V600E}$ cells (Nthy/V600E) were added to the top compartments (8×10^4 cells per well). The impedance data, reported as cell index and proportional to the area of the bottom electrodes covered by migrated/invasive cells, were collected every 15 min. The percentage of invasion was calculated as the ratio between the invasive cells and the migrated cells (8).

Gene expression microarray. Cells were cultured in 100-mm dishes until confluent monolayers were reached. Total RNA was extracted using the easy-spin (DNA free) Total RNA Extraction kit (iNtRON Biotechnology, Seoul, Korea) and quantified using a Nanodrop ND-1000 spectrophotometer (NanoDrop, Wilmington, DE, USA). Microarray services were provided by Macrogen (Macrogen Inc., Seoul, Korea) using the Illumina HumanHT-12 v4 Expression BeadChip (Illumina, Inc., San Diego, CA, USA). Total RNA was amplified and purified using the TargetAmp-Nano Labeling kit for Illumina Expression BeadChip (EPICENTRE, Madison, WI, USA) to yield biotinylated cRNA according to the manufacturer's instructions. Briefly, 500 ng of total RNA was reverse-transcribed to cDNA using a T7 oligo (dT) primer. Second-strand cDNA was synthesized, *in vitro*-transcribed, and labeled with biotin-NTP. After purification, the cRNA was quantified using the ND-1000 Spectrophotometer (NanoDrop, Wilmington, MA, USA). Labeled cRNA samples (750 ng) were hybridized to each Human HT-12 v4.0 Expression Beadchip for 17 h at 58˚C according to the manufacturer's instructions (Illumina, Inc., San Diego, CA, USA). Detection of the array signal was carried out using Amersham fluorolink streptavidin-Cy3 (GE Healthcare Bio-Sciences, Little Chalfont, UK) following the bead array manual. Arrays were scanned with an Illumina bead array reader confocal scanner according to the manufacturer's instructions.

Statistical methods for microarray data analysis. Microarray data were analyzed with two groups based on the $BRAF^{V600E}$ mutation status. The "Wild-type BRAF" group consisted of two Nthy/WT cultures, and the "Mutant-type BRAF" group consisted of two Nthy/V600E cultures. All statistical analyses were performed using R version 3.2 (9). Raw data derived from the Illumina Genome Studio version 2011.1 and Gene Expression Module version 1.9.0 were transformed

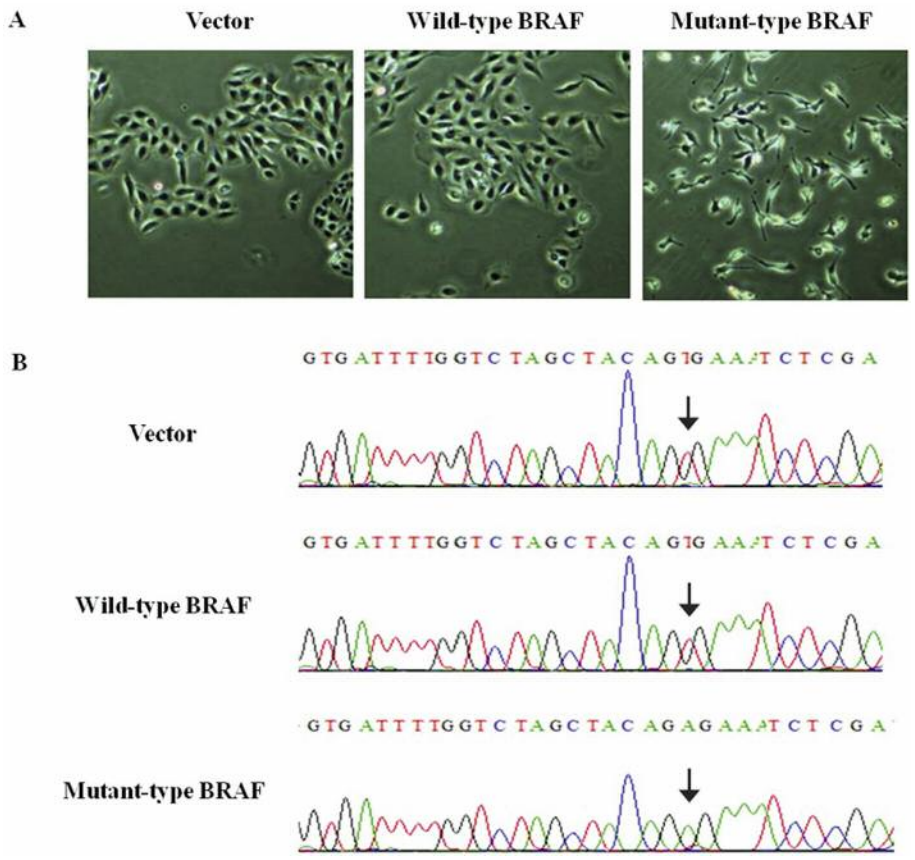

Figure 1. *Cellular morphology and BRAF sequences in Nthy/Vector, Nthy/WT, and Nthy/V600E cells. A: Cells photographed under light microscopy (40×). B: BRAF exon 15 sequences in Nthy/Vector, Nthy/WT, and Nthy/V600E cells.*

into a "LumiBatch" object using “Lumi R package” version 1.1.0. (10). Variance stabilization of gene expression counts was performed using the variance-stabilizing transformation (VST) method. (11). Quantile normalization method was applied to gene expression data after VST. Packages “Annotate" and “IlluminaHumanv4.db” were used for microarray chip probe annotation, provided by bioconductor (http://www.bioconductor.org). To find differentially expressed genes (DEGs), moderated *t*-test using the “Limma” was applied (12). The Benjamini-Hochberg (BH) method was applied to correct false positive rate from multiple comparisons. $p<0.05$ after BH correction was considered statistically significant. A log fold change value of 2 was used as the cutoff to identify significant DEGs. Based on the DEGs identified from limma, "GO stat” package was used for gene ontology (GO) analysis (13). In the gene ontology test, false discover rate (FDR) corrected p-value under 0.01 was considered statistically significant. Pathway analysis using up-regulated DEGs in Nthy/BRAF cells was performed by Database for Annotation, Visualization and Integrated Discovery (DAVID) v6.7 (14).

Results

Effect of BRAF gene transduction into Nthy cells. Nthy cells were stably transfected with empty vector, wild-type *BRAF*, or *BRAF*^{V600E} and named Nthy/Vector, Nthy/WT, and Nthy/V600E, respectively. The cell morphology of the Nthy/Vector and Nthy/WT cells was similar to that of the parental Nthy-ori 3-1 cells; however, Nthy/V600E cells had a spindle transformed shape, as shown in Figure 1A.

BRAF gene sequences were confirmed by Sanger sequencing. As shown in Figure 1B, the *BRAF* exon 15 sequences of Nthy/Vector and Nthy/WT cells were normal. Nthy/V600E cells, however, had a T>A mutation at position 1799. This result shows that the *BRAF*^{V600E} recombinant plasmid was successfully constructed and the *BRAF*^{V600E} expression level in Nthy-ori 3-1 cells surpassed that of the original wild-type *BRAF*.

By flow cytometry (Figure 2A), GFP showed a similar peak fluorescence intensity in Nthy/Vector, Nthy/WT, and Nthy/V600E cells, indicating similar BRAF protein levels. The intensity of p-ERK was increased in Nthy/V600E cells compared to Nthy/Vector or Nthy/WT cells (Figure 2A). Increased p-ERK was also confirmed by western blot (Figure 2B).

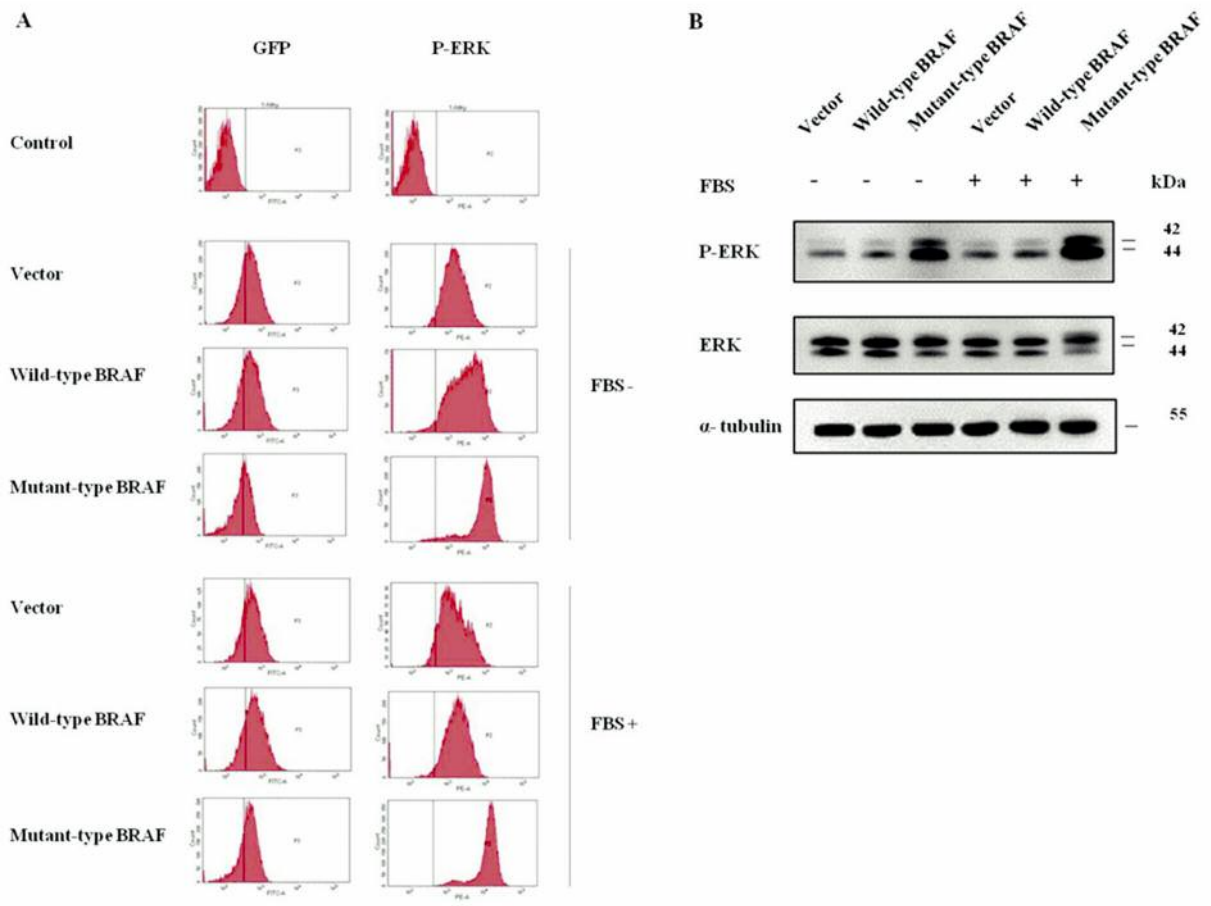

Figure 2. *Phosphorylation level of ERK in Nthy/Vector, Nthy/WT, and Nthy/V600E cells. A: Phosphorylation level of ERK by flow cytometry. Cells were cultured with or without FBS for 24 h. Control: Nthy-ori 3.1 cells cultured with FBS. B: Protein expression levels of phosphorylated ERK and total ERK by western blotting. Cells were cultured with or without FBS for 24 h. α-Tubulin served as a loading control.*

Increased anchorage-independent growth and invasion in Nthy/V600E cells. Soft-agar assay results estimating anchorage-independent growth are illustrated in Figure 3. The number of colonies observed was higher in Nthy/V600E cells than in Nthy/Vector or Nthy/WT cells. Treatment with PLX4032, a potent *BRAF*^{V600E} kinase inhibitor, inhibited colony growth, but the effect was small in Nthy/Vector or Nthy/WT cells; however, colony formation was decreased in a concentration-dependent manner in Nthy/V600E cells. In the invasion assay, the invasion/migration ratio was increased in Nthy/V600E cells, but not in Nthy/WT and control cells (Figure 4). This result indicates that Nthy/V600E cells are highly invasive compared to Nthy/Vector or Nthy/WT cells. Altogether, Nthy/V600E cells have increased anchorage-independent growth and a stronger invasive potential compared to Nthy/Vector or Nthy/WT cells.

Gene expression microarray. In total, 2,441 genes were differentially expressed at a higher level in Nthy/V600E cells compared to Nthy/WT cells (BH $p<0.05$ and absolute log fold change >0). Forty-four genes were considered as significantly up-regulated DEGs in Nthy/V600E cells compared to Nthy/WT (BH p-value <0.05 and absolute log fold change >2, Table I. Among them, the top 20 up-regulated genes in Nthy/V600E cells and their ontology terms are listed on Table II. Their gene ontologies included carcinogenesis-related terms such as "MAPK pathway activation (*IL1B, DCLK1, TRIB1*)", "Wnt receptor signaling pathway (*SFRP1*)", "TOR signaling (*AGPAT9*)", "inflammation (*PLA2G7, NT5E*)", "cell proliferation (*IL24*), migration (*SERPINE1*), adhesion (*ITGA2*)", and "apoptosis (*G0S2, PHLDA1*)". 2,724 genes were differentially expressed at a lower level in Nthy/V600E cells compared to Nthy/WT cells. Forty-eight genes were considered significantly down-regulated DEGs. Information of down-regulated DEGs were also listed in Table III.

In GO analysis, 210 gene ontologies were enriched in Nthy/V600E cells (Table IV). Enriched GO terms in Nthy/V600E cells that were concordant with our functional

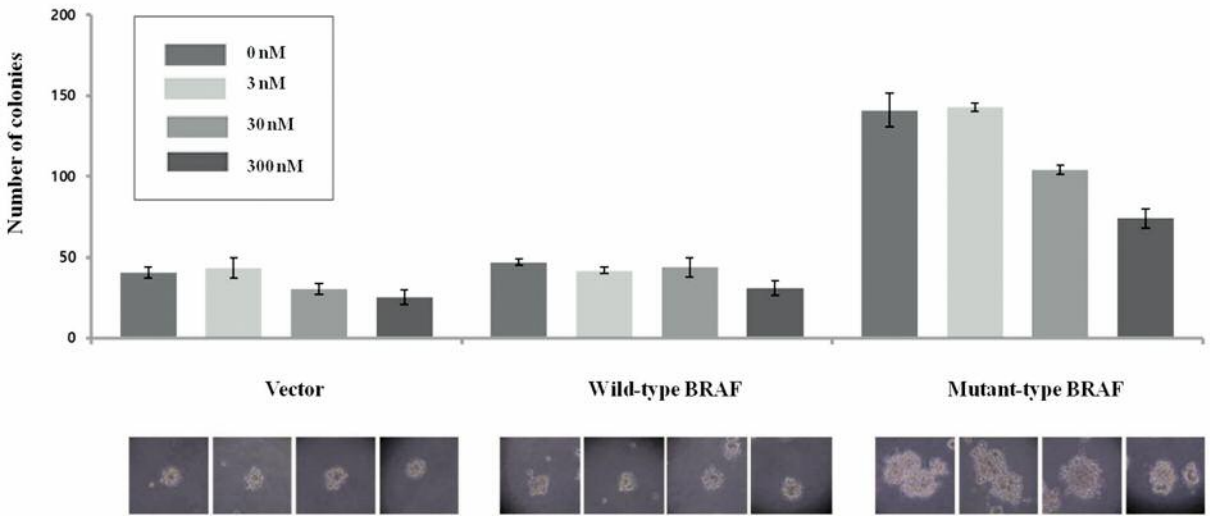

Figure 3. *Colony formation in Nthy/Vector, Nthy/WT, and Nthy/V600E cells. Cells were grown in a 3-dimensional agar gel and treated with PLX4032, a potent inhibitor of BRAF*^{V600E} *kinase. Representative images are shown.*

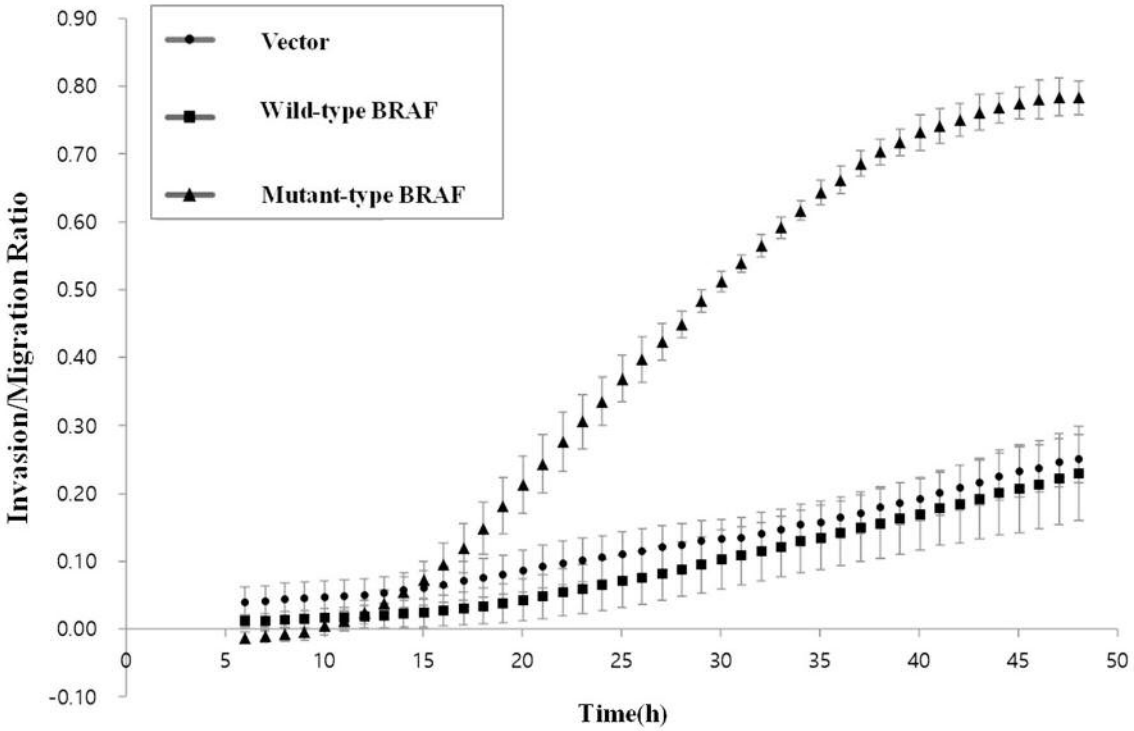

Figure 4. *Invasion/migration ratio in Nthy/Vector, Nthy/WT, and Nthy/V600E cells. The coverage of bottom electrodes, which is proportional to the number of cells that have invaded through a Matrigel-coated porous membrane or migrated through an uncoated porous membrane, was measured using a Real Time Cell Analyzer. The percentage of invasion was calculated by the ratio between the invasive cells and the migrated cells.*

analysis were as follows: morphological change to spindle shape ("cell morphogenesis"), increased cell growth in soft agar ("cell differentiation", "cell growth", "cell motility", "cell migration"), increased invasion ("cell motility", "cell adhesion"), overexpression of p-ERK ("ERK1 and ERK2 cascade", "MAPK cascade").

Table I. *Up-regulated DEGs in Nthy/V600E cells.*

Probe ID	Gene symbol	Gene name	Log fold change	Average expression	*p*-Value	FDR *q*-Value
ILMN_1775501	*IL1B*	Interleukin 1, beta	4,826	10,380	<0.001	<0.001
ILMN_3237961	*ANO1*	Anoctamin 1, calcium activated chloride channel	3,701	9,876	<0.001	<0.001
ILMN_1725387	*TMEM200A*	Transmembrane protein 200A	2,988	10,516	<0.001	<0.001
ILMN_1705579	*MPP4*	Membrane protein, palmitoylated 4 (MAGUK p55 subfamily member 4)	3,260	9,842	<0.001	<0.001
ILMN_1717909	*ANO1*	Anoctamin 1, calcium activated chloride channel	3,538	9,827	<0.001	<0.001
ILMN_1794875	*AGPAT9*	1-acylglycerol-3-phosphate O-acyltransferase 9	2,601	10,072	<0.001	<0.001
ILMN_2149164	*SFRP1*	Secreted frizzled-related protein 1	3,553	13,181	<0.001	<0.001
ILMN_1812926	*ANTXR2*	Anthrax toxin receptor 2	2,847	10,179	<0.001	<0.001
ILMN_1793410	*SNTB1*	Syntrophin, beta 1 (dystrophin-associated protein A1, 59kDa, basic component 1)	2,591	9,237	<0.001	<0.001
ILMN_1701195	*PLA2G7*	Phospholipase A2, group VII (platelet-activating factor acetylhydrolase, plasma)	2,371	9,366	<0.001	<0.001
ILMN_1748840	*CALB2*	Calbindin 2	2,461	9,594	<0.001	<0.001
ILMN_1691747	*KHDRBS3*	KH domain containing, RNA binding, signal transduction associated 3	3,236	10,295	<0.001	<0.001
ILMN_1715684	*LAMB3*	Laminin, beta 3	2,360	11,800	<0.001	<0.001
ILMN_1655595	*SERPINE2*	Serpin peptidase inhibitor, clade E (nexin, plasminogen activator inhibitor type 1), member 2	3,634	13,116	<0.001	<0.001
ILMN_1697220	*NT5E*	5'-nucleotidase, ecto (CD73)	2,156	10,979	<0.001	<0.001
ILMN_1774685	*IL24*	Interleukin 24	2,986	9,693	<0.001	<0.001
ILMN_1758164	*STC1*	Stanniocalcin 1	2,229	12,356	<0.001	<0.001
ILMN_1665792	*ITGA2*	Integrin, alpha 2 (CD49B, alpha 2 subunit of VLA-2 receptor)	2,303	9,585	<0.001	<0.001
ILMN_1687978	*PHLDA1*	Pleckstrin homology-like domain, family A, member 1	2,384	12,260	<0.001	<0.001
ILMN_2165354	*DCLK1*	Doublecortin-like kinase 1	2,705	9,957	<0.001	<0.001
ILMN_1691846	*G0S2*	G0/G1 switch 2	2,911	10,162	<0.001	<0.001
ILMN_2091310	*ANO1*	Anoctamin 1, calcium activated chloride channel	4,339	10,030	<0.001	<0.001
ILMN_1803811	*TRIB1*	Tribbles pseudokinase 1	2,005	9,794	<0.001	<0.001
ILMN_1669046	*FOXQ1*	Forkhead box Q1	2,820	9,534	<0.001	<0.001
ILMN_1678170	*MME*	Membrane metallo-endopeptidase	2,062	9,259	<0.001	<0.001
ILMN_1792455	*TMEM158*	Transmembrane protein 158 (gene/pseudogene)	3,045	13,295	<0.001	<0.001
ILMN_1765558	*NPAS2*	Neuronal PAS domain protein 2	2,031	9,174	<0.001	<0.001
ILMN_3248511	*FAM167A*	Family with sequence similarity 167, member A	2,874	10,693	<0.001	<0.001
ILMN_1703178	*SCG2*	Secretogranin II	3,241	10,381	<0.001	<0.001
ILMN_1687213	*FAM167A*	Family with sequence similarity 167, member A	2,878	11,181	<0.001	0.001
ILMN_2337974	*PKIA*	Protein kinase (cAMP-dependent, catalytic) inhibitor alpha	2,233	9,016	<0.001	0.001
ILMN_1678143	*ARHGDIB*	Rho GDP dissociation inhibitor (GDI) beta	2,179	9,331	<0.001	0.001
ILMN_2086105	*SPRY4*	Sprouty homolog 4 (Drosophila)	2,731	10,360	<0.001	0.001
ILMN_1699695	*TNFRSF21*	Tumor necrosis factor receptor superfamily, member 21	2,407	10,210	<0.001	0.001
ILMN_2348788	*CD44*	CD44 molecule (Indian blood group)	2,231	11,828	<0.001	0.001
ILMN_1778625	*CD44*	CD44 molecule (Indian blood group)	2,175	9,664	<0.001	0.001
ILMN_1760412	*SHISA2*	Shisa family member 2	2,452	10,058	<0.001	0.001
ILMN_2184373	*CXCL8*	Chemokine (C-X-C motif) ligand 8	2,578	11,433	<0.001	0.002
ILMN_1801616	*EMP1*	Epithelial membrane protein 1	2,660	13,062	<0.001	0.002
ILMN_2396020	*DUSP6*	Dual specificity phosphatase 6	2,434	10,506	<0.001	0.002
ILMN_1660067	*KRTAP2-3*	Keratin associated protein 2-3	2,167	9,526	<0.001	0.002
ILMN_3266606	*FABP5*	Fatty acid binding protein 5 (psoriasis-associated)	2,093	11,487	<0.001	0.002
ILMN_2089329	*SPRY2*	Sprouty homolog 2 (Drosophila)	2,053	12,185	<0.001	0.003
ILMN_1666733	*CXCL8*	Chemokine (C-X-C motif) ligand 8	2,276	10,331	<0.001	0.004

Significantly enriched pathways by up-regulated genes in Nthy/V600E are listed in Table V. Apoptosis, small cell lung cancer, pathways in cancer, colorectal cancer, cell cycle, and p53 signaling pathway were enriched in Nthy/V600E cells, but not in Nthy/WT cells. This result shows that the activation of cancer-related genes and pathways is increased in Nthy/BRAF cells compared to Nthy/WT cells.

Table II. *Top 20 up-regulated DEGs and their gene ontology terms in Nthy/V600E mutant cells with growth factor treatment.*

Genes	Full name	Log FC	BH *p*-value	Gene ontology terms
IL1B	Interleukin 1, Beta	4,826	<0.001	Activation of MAPK activity
ANO1	Anoctamin 1, Calcium-Activated Chloride Channel	4,339	<0.001	Ion transmembrane transport, multicellular organismal development
SERPINE2	Serpin Peptidase Inhibitor, Clade E, Member 2	3,634	<0.001	Regulation of cell migration
SFRP1	Secreted Frizzled-Related Protein 1	3,553	<0.001	Wnt receptor signaling pathway, regulation of peptidyl-tyrosine phosphorylation
MPP4	Membrane Protein, Palmitoylated 4	3,26	<0.001	Protein localization to synapse
KHDRBS3	Kh Domain-Containing, Rna-Binding, Signal Transduction-Associated 3	3,236	<0.001	Regulation of transcription
TMEM200A	Transmembrane Protein 200A	2,988	<0.001	Integral to membrane
IL24	Interleukin 24	2,986	<0.001	Regulation of cell proliferation
G0S2	G0/G1 Switch 2	2,911	<0.001	Regulation of apoptotic signaling pathway
ANTXR2	Anthrax Toxin Receptor 2	2,847	<0.001	Integral to membrane
FOXQ1	Forkhead Box Q1	2,82	<0.001	Tissue development
DCLK1	Doublecortin-Like Kinase 1	2,705	<0.001	Protein kinase activity, phosphorylation
AGPAT9	1-Acylglycerol-3-Phosphate O-Acyltransferase 9	2,601	<0.001	Regulation of TOR signaling
SNTB1	Syntrophin, Beta 1	2,591	<0.001	Protein binding, phospholipid binding
CALB2	Calbindin 2	2,461	<0.001	Calcium ion binding, cytoplasm, gap junction
PHLDA1	Pleckstrin Homology-Like Domain, Family A, Member 1	2,384	<0.001	Protein binding, phospholipid binding, apoptotic process
PLA2G7	Phospholipase A2, Group Vii	2,371	<0.001	Regulation of inflammatory response
LAMB3	Laminin, Beta 3	2,36	<0.001	Structural molecule activity, extracellular matrix organization
ITGA2	Integrin, Alpha 2	2,303	<0.001	Cell-matrix adhesion, integrin-mediated signaling pathway
STC1	Stanniocalcin 1	2,229	<0.001	Cell surface receptor signaling pathway

Discussion

The characteristics of Nthy/V600E cells were as follows: shape change to spindle type, increased anchorage-independent growth and invasion potential, increased p-ERK and overexpression of MAPK-related genes, and enrichment of cancer-related pathways.

The cell shape change in Nthy/V600E may be the result of epithelial-mesenchymal transition (EMT) induced by the *BRAF* mutation. A previous study reported that thyroid cancer cells differed in shape from wild-type epithelial thyroid cells and appeared spindle-shaped in *BRAF*^{V600E} mice. The hallmark of EMT is the down-regulation of E-cadherin and up-regulation of vimentin expression. A significant loss of E-cadherin gene expression and an increase in vimentin gene expression were seen in *BRAF*^{V600E} thyroid tumors compared to normal thyroid (15). EMT is a normal morphological event during embryonic development, tissue remodeling, and wound-healing but also occurs in neoplastic cells, especially in metastases (16). *BRAF*^{V600E} expression in the rat thyroid PCCL3 cell line promotes EMT and invasion through an autocrine transforming growth factor (TGF)-β loop (1). In concordance with the previous literature, genes associated with EMT, *i.e.*, vimentin, were highly expressed in Nthy/V600E cells compared to Nthy/WT cells in microarray experiments (data not shown). We plan to perform further functional studies to validate this observation.

The oncogenic BRAF protein is always phosphorylated to activate ERK signaling. The mechanism of phosphorylation of oncogenic BRAF has been described by Wan et al. Normal BRAF is maintained in a conformational state, where the ATP-binding domain is bound to the phosphorylation domain. In mutant BRAF, the combination is scattered and activates to be phosphorylation (17). PLX4032 is a selective *BRAF*^{V600E} inhibitor. In cells harboring *BRAF*^{V600E}, PLX4032 inhibits MAP kinase signaling effectively and suppresses phosphorylation of ERK. In tumor xenograft models of *BRAF*^{V600E} melanoma, PLX4032 suppresses the proliferation of tumor cells and improves the survival of animals in a dose-dependent manner (18,19). Likewise, PLX4032 inhibited anchorage-independent growth in Nthy/V600E cells in the present study (Figure 3), suggesting that *BRAF*^{V600E} may play an important role in anchorage-independent growth. In another study using PCCL3 rat thyroid cell lines with doxycycline-inducible expression of *BRAF*^{V600E}, *BRAF*^{V600E} protein expression and ERK phosphorylation were doxycycline dose-dependent (6, 20). In another study using PCCL3 cells to

Table III. *Down-regulated DEGs in Nthy/V600E cells.*

Probe ID	Gene symbol	Gene name	Log fold change	Average expression	*p*-Value	FDR *q*-Value
ILMN_2327860	*MAL*	Mal, T-cell differentiation protein	–3,377	9,635	<0.001	<0.001
ILMN_1760247	*CD70*	CD70 molecule	–3,322	10,835	<0.001	<0.001
ILMN_1680874	*TUBB2B*	Tubulin, beta 2B class IIb	–4,890	10,909	<0.001	<0.001
ILMN_1898518	*GFRA1*	GDNF family receptor alpha 1	–3,092	10,379	<0.001	<0.001
ILMN_3246401	*AIF1L*	Allograft inflammatory factor 1-like	–3,438	11,427	<0.001	<0.001
ILMN_2201678	*FSTL1*	Follistatin-like 1	–2,703	11,887	<0.001	<0.001
ILMN_1815057	*PDGFRB*	Platelet-derived growth factor receptor, beta polypeptide	–3,247	9,793	<0.001	<0.001
ILMN_1693338	*CYP1B1*	Cytochrome P450, family 1, subfamily B, polypeptide 1	–3,376	9,928	<0.001	<0.001
ILMN_1685441	*ASAP3*	ArfGAP with SH3 domain, ankyrin repeat and PH domain 3	–2,535	9,920	<0.001	<0.001
ILMN_1730995	*AFAP1L2*	Actin filament associated protein 1-like 2	–2,712	10,116	<0.001	<0.001
ILMN_1694840	*MATN2*	Matrilin 2	–2,716	11,365	<0.001	<0.001
ILMN_1778668	*TAGLN*	Transgelin	–4,406	11,177	<0.001	<0.001
ILMN_1698732	*PALLD*	Palladin, cytoskeletal associated protein	–2,199	10,762	<0.001	<0.001
ILMN_1730229	*CGNL1*	Cingulin-like 1	–2,505	10,244	<0.001	<0.001
ILMN_1653028	*COL4A1*	Collagen, type IV, alpha 1	–2,178	11,638	<0.001	<0.001
ILMN_1770725	*AIF1L*	Allograft inflammatory factor 1-like	–2,012	9,189	<0.001	<0.001
ILMN_1652631	*GLIPR2*	GLI pathogenesis-related 2	–2,622	10,708	<0.001	<0.001
ILMN_1652246	*NACAD*	NAC alpha domain containing	–2,584	9,553	<0.001	<0.001
ILMN_1706505	*COL5A1*	Collagen, type V, alpha 1	–2,531	12,203	<0.001	<0.001
ILMN_1796734	*SPARC*	Secreted protein, acidic, cysteine-rich (osteonectin)	–3,232	12,415	<0.001	<0.001
ILMN_1666503	*DENND2A*	DENN/MADD domain containing 2A	–2,971	10,237	<0.001	<0.001
ILMN_1796423	*CLIC3*	Chloride intracellular channel 3	–2,415	9,157	<0.001	<0.001
ILMN_1701308	*COL1A1*	Collagen, type I, alpha 1	–3,699	12,082	<0.001	<0.001
ILMN_2319424	*GYG2*	Glycogenin 2	–2,225	9,348	<0.001	<0.001
ILMN_2386982	*PRKCZ*	Protein kinase C, zeta	–2,363	9,393	<0.001	<0.001
ILMN_2384745	*PSG4*	Pregnancy specific beta-1-glycoprotein 4	–2,280	9,367	<0.001	<0.001
ILMN_1724658	*BNIP3*	BCL2/adenovirus E1B 19kDa interacting protein 3	–2,052	13,370	<0.001	<0.001
ILMN_3307729	*CXXC5*	CXXC finger protein 5	–2,102	10,971	<0.001	<0.001
ILMN_2400935	*TAGLN*	Transgelin	–2,549	9,330	<0.001	<0.001
ILMN_1811238	*ALPK2*	Alpha-kinase 2	–2,762	9,362	<0.001	<0.001
ILMN_2190084	*VAMP8*	Vesicle-associated membrane protein 8	–2,063	9,677	<0.001	<0.001
ILMN_1788955	*PDLIM1*	PDZ and LIM domain 1	–2,151	11,140	<0.001	<0.001
ILMN_1663866	*TGFBI*	Transforming growth factor, beta-induced, 68kDa	–2,069	14,266	<0.001	0.001
ILMN_1680738	*NREP*	Neuronal regeneration related protein	–2,553	11,219	<0.001	0.001
ILMN_2093343	*PLAC8*	Placenta-specific 8	–2,619	10,583	<0.001	0.001
ILMN_2353161	*MSLN*	Mesothelin	–2,182	9,738	<0.001	0.001
ILMN_1653292	*PFKFB4*	6-phosphofructo-2-kinase/fructose-2,6-biphosphatase 4	–2,128	10,076	<0.001	0.001
ILMN_2047511	*ADAP1*	ArfGAP with dual PH domains 1	–2,161	9,819	<0.001	0.001
ILMN_1729117	*COL5A2*	Collagen, type V, alpha 2	–2,285	9,747	<0.001	0.001
ILMN_1812031	*PALM*	Paralemmin	–2,319	10,366	<0.001	0.001
ILMN_1798360	*ACKR3*	Atypical chemokine receptor 3	–2,775	9,252	<0.001	0.001
ILMN_1784294	*CPA4*	Carboxypeptidase A4	–3,510	10,662	<0.001	0.001
ILMN_1801442	*KRT81*	Keratin 81, type II	–3,719	10,138	<0.001	0.001
ILMN_1790689	*CRISPLD2*	Cysteine-rich secretory protein LCCL domain containing 2	–2,792	9,620	<0.001	0.001
ILMN_1763382	*NPPB*	Natriuretic peptide B	–4,306	10,179	<0.001	0.002
ILMN_1653026	*PLAC8*	Placenta-specific 8	–2,243	9,845	<0.001	0.002
ILMN_2186983	*ANXA8L1*	Annexin A8-like 1	–2,030	9,015	<0.001	0.003
ILMN_1746085	*IGFBP3*	Insulin-like growth factor binding protein 3	–2,133	9,455	<0.001	0.005

obtain doxycycline-inducible expression of BRAFV600E, *BRAF*^{V600E} induced invasion through Matrigel (21). In a study using the human PTC-derived cell lines KAT5 and KAT10 harboring a heterozygous *BRAF*^{V600E} mutation, stable knockdown of *BRAF* using *BRAF* small interfering RNA (siRNA) suppressed anchorage-independent colony formation in soft agar (22). Our results are consistent with previous reports of thyrocyte cell lines. The clinical features of *BRAF*^{V600E}, generally thought to be associated with aggressive thyroid cancers, also correlate with our *in vitro* data.

Table IV. *Gene ontologies (GO) enriched in Nthy/V600E cells treated with growth factor.*

GO ID	GO Term	*p*-Value	Numbers of matched genes	Numbers of total genes in GO
GO:0008219	Cell death	<0.001	62	1843
GO:0060560	Developmental growth involved in morphogenesis	<0.001	17	166
GO:0016265	Death	<0.001	62	1847
GO:0009653	Anatomical structure morphogenesis	<0.001	74	2438
GO:0007155	Cell adhesion	<0.001	50	1344
GO:0022610	Biological adhesion	<0.001	50	1351
GO:0010941	Regulation of cell death	<0.001	51	1406
GO:0012501	Programmed cell death	<0.001	58	1755
GO:0030155	Regulation of cell adhesion	<0.001	29	561
GO:0006915	Apoptotic process	<0.001	57	1737
GO:0043067	Regulation of programmed cell death	<0.001	48	1337
GO:0048585	Negative regulation of response to stimulus	<0.001	45	1219
GO:0060429	Epithelium development	<0.001	41	1049
GO:0042981	Regulation of apoptotic process	<0.001	47	1328
GO:0008283	Cell proliferation	<0.001	57	1809
GO:0042127	Regulation of cell proliferation	<0.001	48	1397
GO:0040011	Locomotion	<0.001	51	1546
GO:0009888	Tissue development	<0.001	54	1687
GO:0009968	Negative regulation of signal transduction	<0.001	38	986
GO:0032502	Developmental process	<0.001	119	5301
GO:0016477	Cell migration	<0.001	40	1077
GO:0048856	Anatomical structure development	<0.001	109	4706
GO:0009605	Response to external stimulus	<0.001	60	2047
GO:0048522	Positive regulation of cellular process	<0.001	98	4116
GO:0048589	Developmental growth	<0.001	22	404
GO:0006928	Movement of cell or subcellular component	<0.001	52	1663
GO:0048583	Regulation of response to stimulus	<0.001	83	3275
GO:0043065	Positive regulation of apoptotic process	<0.001	26	547
GO:0007275	Multicellular organismal development	<0.001	104	4483
GO:0044767	Single-organism developmental process	<0.001	116	5217
GO:0043068	Positive regulation of programmed cell death	<0.001	26	552
GO:0023057	Negative regulation of signaling	<0.001	39	1079
GO:0048519	Negative regulation of biological process	<0.001	98	4157
GO:0010648	Negative regulation of cell communication	<0.001	39	1086
GO:0060602	Branch elongation of an epithelium	<0.001	6	20
GO:0003401	Axis elongation	<0.001	7	32
GO:0048468	Cell development	<0.001	56	1906
GO:0042325	Regulation of phosphorylation	<0.001	42	1240
GO:0008285	Negative regulation of cell proliferation	<0.001	27	609
GO:0048513	Organ development	<0.001	74	2845
GO:0010942	Positive regulation of cell death	<0.001	26	573
GO:0048870	Cell motility	<0.001	40	1159
GO:0051674	Localization of cell	<0.001	40	1159
GO:0006468	Protein phosphorylation	<0.001	46	1439
GO:0001763	Morphogenesis of a branching structure	<0.001	15	210
GO:0048729	Tissue morphogenesis	<0.001	26	584
GO:0019220	Regulation of phosphate metabolic process	<0.001	46	1447
GO:0040007	Growth	<0.001	33	866
GO:0022407	Regulation of cell-cell adhesion	<0.001	19	336
GO:0035295	Tube development	<0.001	26	587
GO:0051174	Regulation of phosphorus metabolic process	<0.001	46	1460
GO:0009790	Embryo development	<0.001	35	969
GO:1902532	Negative regulation of intracellular signal transduction	<0.001	20	379
GO:0048731	System development	<0.001	92	3928
GO:0030154	Cell differentiation	<0.001	83	3424
GO:0001932	Regulation of protein phosphorylation	<0.001	36	1023
GO:0009966	Regulation of signal transduction	<0.001	67	2549

Table IV. *Continued*

Table IV. *Continued*

GO ID	GO Term	*p*-Value	Numbers of matched genes	Numbers of total genes in GO
GO:0002009	Morphogenesis of an epithelium	<0.001	22	458
GO:0044763	Single-organism cellular process	<0.001	203	11513
GO:0048518	Positive regulation of biological process	<0.001	107	4851
GO:0061138	Morphogenesis of a branching epithelium	<0.001	14	199
GO:0006469	Negative regulation of protein kinase activity	<0.001	14	201
GO:0048869	Cellular developmental process	<0.001	86	3640
GO:0048523	Negative regulation of cellular process	<0.001	89	3818
GO:0051246	Regulation of protein metabolic process	<0.001	58	2123
GO:0006935	Chemotaxis	<0.001	27	674
GO:0042330	Taxis	<0.001	27	674
GO:0072001	Renal system development	<0.001	16	271
GO:0009887	Organ morphogenesis	<0.001	32	888
GO:0016049	Cell growth	<0.001	20	409
GO:0040012	Regulation of locomotion	<0.001	26	641
GO:0001655	Urogenital system development	<0.001	17	310
GO:0033673	Negative regulation of kinase activity	<0.001	14	215
GO:0048598	Embryonic morphogenesis	<0.001	24	569
GO:0001933	Negative regulation of protein phosphorylation	<0.001	16	284
GO:0042326	Negative regulation of phosphorylation	<0.001	18	353
GO:0042221	Response to chemical	<0.001	86	3731
GO:0060562	Epithelial tube morphogenesis	<0.001	17	322
GO:0035556	Intracellular signal transduction	<0.001	59	2243
GO:0098602	Single organism cell adhesion	<0.001	27	706
GO:0016337	Single organismal cell-cell adhesion	<0.001	26	665
GO:2000145	Regulation of cell motility	<0.001	24	585
GO:0001704	Formation of primary germ layer	<0.001	10	114
GO:0048754	Branching morphogenesis of an epithelial tube	<0.001	12	167
GO:0023051	Regulation of signaling	<0.001	70	2843
GO:0035239	Tube morphogenesis	<0.001	18	361
GO:0007369	Gastrulation	<0.001	12	169
GO:0010646	Regulation of cell communication	<0.001	70	2856
GO:0016310	Phosphorylation	<0.001	52	1898
GO:0048646	Anatomical structure formation involved in morphogenesis	<0.001	34	1024
GO:0030334	Regulation of cell migration	<0.001	23	554
GO:0044267	Cellular protein metabolic process	<0.001	92	4125
GO:0048588	Developmental cell growth	<0.001	10	119
GO:0080134	Regulation of response to stress	<0.001	34	1034
GO:0022408	Negative regulation of cell-cell adhesion	<0.001	10	120
GO:0070887	Cellular response to chemical stimulus	<0.001	60	2336
GO:0060548	Negative regulation of cell death	<0.001	30	861
GO:0006793	Phosphorus metabolic process	<0.001	68	2781
GO:0032268	Regulation of cellular protein metabolic process	<0.001	52	1926
GO:0048584	Positive regulation of response to stimulus	<0.001	48	1726
GO:0051270	Regulation of cellular component movement	<0.001	25	654
GO:0006796	Phosphate-containing compound metabolic process	<0.001	67	2737
GO:0000904	Cell morphogenesis involved in differentiation	<0.001	29	832
GO:0048699	Generation of neurons	<0.001	39	1298
GO:0019538	Protein metabolic process	<0.001	101	4736
GO:0010563	Negative regulation of phosphorus metabolic process	<0.001	20	464
GO:0045936	Negative regulation of phosphate metabolic process	<0.001	20	464
GO:0042493	Response to drug	<0.001	18	394
GO:0043549	Regulation of kinase activity	<0.001	27	764
GO:0001822	Kidney development	<0.001	14	256
GO:0043409	Negative regulation of MAPK cascade	<0.001	10	134
GO:0043069	Negative regulation of programmed cell death	<0.001	28	812
GO:0007162	Negative regulation of cell adhesion	<0.001	12	193
GO:0044707	Single-multicellular organism process	<0.001	124	6230

Table IV. *Continued*

Table IV. *Continued*

GO ID	GO Term	*p*-Value	Numbers of matched genes	Numbers of total genes in GO
GO:0044092	Negative regulation of molecular function	<0.001	31	952
GO:0030182	Neuron differentiation	<0.001	36	1193
GO:0051247	Positive regulation of protein metabolic process	<0.001	37	1243
GO:0051239	Regulation of multicellular organismal process	<0.001	56	2221
GO:0072073	Kidney epithelium development	<0.001	10	140
GO:0031399	Regulation of protein modification process	<0.001	38	1298
GO:0007417	Central nervous system development	<0.001	28	831
GO:0050680	Negative regulation of epithelial cell proliferation	<0.001	9	114
GO:2000026	Regulation of multicellular organismal development	<0.001	40	1403
GO:0022603	Regulation of anatomical structure morphogenesis	<0.001	27	792
GO:1902531	Regulation of intracellular signal transduction	<0.001	44	1608
GO:0007165	Signal transduction	<0.001	106	5162
GO:0033993	Response to lipid	<0.001	25	711
GO:0043066	Negative regulation of apoptotic process	<0.001	27	803
GO:0014070	Response to organic cyclic compound	<0.001	25	716
GO:0022008	Neurogenesis	<0.001	39	1374
GO:0045859	Regulation of protein kinase activity	<0.001	25	719
GO:0061564	Axon development	<0.001	22	592
GO:0044700	Single organism signaling	<0.001	113	5638
GO:0023052	Signaling	<0.001	113	5640
GO:0032270	Positive regulation of cellular protein metabolic process	<0.001	34	1141
GO:0014812	Muscle cell migration	<0.001	6	50
GO:0048732	Gland development	<0.001	17	395
GO:0050673	Epithelial cell proliferation	<0.001	15	320
GO:0023014	Signal transduction by phosphorylation	<0.001	24	685
GO:0022612	Gland morphogenesis	<0.001	9	124
GO:2000736	Regulation of stem cell differentiation	<0.001	8	98
GO:0007154	Cell communication	<0.001	114	5728
GO:0043407	Negative regulation of MAP kinase activity	<0.001	7	74
GO:0070371	ERK1 and ERK2 cascade	<0.001	11	187
GO:0032989	Cellular component morphogenesis	<0.001	36	1255
GO:0071901	Negative regulation of protein serine/threonine kinase activity	<0.001	9	127
GO:0001525	Angiogenesis	<0.001	17	404
GO:0000165	MAPK cascade	<0.001	23	653
GO:0031175	Neuron projection development	<0.001	27	832
GO:0007409	Axonogenesis	<0.001	21	569
GO:0032501	Multicellular organismal process	<0.001	125	6465
GO:0007492	Endoderm development	<0.001	7	77
GO:0051248	Negative regulation of protein metabolic process	<0.001	27	839
GO:0048608	Reproductive structure development	<0.001	17	410
GO:0050896	Response to stimulus	<0.001	141	7532
GO:0000902	Cell morphogenesis	<0.001	34	1173
GO:0071310	Cellular response to organic substance	<0.001	48	1892
GO:0051093	Negative regulation of developmental process	<0.001	26	798
GO:0051716	Cellular response to stimulus	<0.001	121	6227
GO:0043086	Negative regulation of catalytic activity	<0.001	25	753
GO:0061458	Reproductive system development	<0.001	17	413
GO:0051094	Positive regulation of developmental process	<0.001	30	986
GO:0048863	Stem cell differentiation	<0.001	15	337
GO:0001706	Endoderm formation	<0.001	6	56
GO:0045785	Positive regulation of cell adhesion	<0.001	15	338
GO:0010033	Response to organic substance	<0.001	58	2443
GO:0014910	Regulation of smooth muscle cell migration	<0.001	5	36
GO:0007399	Nervous system development	<0.001	50	2008
GO:0030198	Extracellular matrix organization	<0.001	16	378
GO:0001934	Positive regulation of protein phosphorylation	<0.001	24	715
GO:0043062	Extracellular structure organization	<0.001	16	379

Table IV. *Continued*

Table IV. *Continued*

GO ID	GO Term	*p*-Value	Numbers of matched genes	Numbers of total genes in GO
GO:0051348	Negative regulation of transferase activity	<0.001	14	304
GO:0010604	Positive regulation of macromolecule metabolic process	<0.001	57	2399
GO:0006954	Inflammatory response	<0.001	21	588
GO:0071409	Cellular response to cycloheximide	<0.001	2	2
GO:0032269	Negative regulation of cellular protein metabolic process	<0.001	25	768
GO:0060485	Mesenchyme development	<0.001	11	201
GO:0001568	Blood vessel development	<0.001	20	548
GO:0010562	Positive regulation of phosphorus metabolic process	<0.001	29	955
GO:0045937	Positive regulation of phosphate metabolic process	<0.001	29	955
GO:0072009	Nephron epithelium development	<0.001	8	109
GO:0070373	Negative regulation of ERK1 and ERK2 cascade	<0.001	5	38
GO:0048666	Neuron development	<0.001	29	958
GO:0048864	Stem cell development	<0.001	13	273
GO:0014031	Mesenchymal cell development	<0.001	9	140
GO:0030307	Positive regulation of cell growth	<0.001	8	111
GO:0014033	Neural crest cell differentiation	<0.001	6	60
GO:0051241	Negative regulation of multicellular organismal process	<0.001	27	873
GO:0070372	Regulation of ERK1 and ERK2 cascade	<0.001	10	174
GO:0031589	Cell-substrate adhesion	<0.001	13	278
GO:0031400	Negative regulation of protein modification process	<0.001	17	435
GO:0048812	Neuron projection morphogenesis	<0.001	22	649
GO:0040008	Regulation of growth	<0.001	20	562
GO:1903034	Regulation of response to wounding	<0.001	15	356
GO:0050793	Regulation of developmental process	<0.001	48	1949
GO:0014909	Smooth muscle cell migration	<0.001	5	41
GO:0048514	Blood vessel morphogenesis	<0.001	18	481
GO:0051338	Regulation of transferase activity	<0.001	27	885
GO:0065009	Regulation of molecular function	<0.001	58	2507
GO:0001944	Vasculature development	<0.001	20	568
GO:0006950	Response to stress	<0.001	74	3428
GO:0001558	Regulation of cell growth	<0.001	14	323
GO:0060322	Head development	<0.001	22	658
GO:0007160	Cell-matrix adhesion	<0.001	10	180
GO:0042327	Positive regulation of phosphorylation	<0.001	26	844
GO:0022409	Positive regulation of cell-cell adhesion	<0.001	11	216
GO:0010605	Negative regulation of macromolecule metabolic process	<0.001	48	1970
GO:0007420	Brain development	<0.001	21	622
GO:0065008	Regulation of biological quality	<0.001	69	3160
GO:0071222	Cellular response to lipopolysaccharide	<0.001	8	121

GO analysis of microarrays supported our functional results. DEGs up-regulated in Nthy/V600E cells are associated with cancer-related gene ontologies and pathways, showing that Nthy/V600E cells, but not Nthy/Vector or Nthy/WT cells, have carcinogenic potential.

We searched about the top four up-regulated genes in Nthy/V600E cells analyzed in light of previous research. *IL-1* is a principal component of the interleukin-1 family (23). High-dose IL-1β administration causes broad inflammation and is accompanied by tissue damage and tumor invasiveness (24). *In vitro* analysis of melanocytes and melanoma cell lines showed that $BRAF^{V600E}$ increases, while $BRAF^{V600E}$ inhibition reduces, the transcription of IL-1α and IL-1β (25, 26). In human thyrocytes, IL-1β alters the expression and localization of junction proteins (27). IL-1β induces the activation of cAMP responsive element-binding protein (CREB) through ERK1/2 signaling, and this mechanism was associated with poor prognosis in gastric carcinoma, non-small cell lung cancer, and breast cancer patients in previous reports (28-30).

The *ANO1* gene encodes the protein ANO1 [transmembrane member 16A (TMEM16A)], a voltage-sensitive calcium-activated chloride channel (31). In a study in head and neck squamous cell carcinoma, *ANO1* overexpression significantly promoted anchorage-independent growth *in vitro,* whereas loss of *ANO1* resulted in inhibition of tumor growth. *ANO1*-induced cell proliferation and tumor growth were accompanied by an

Table V. *Pathways enriched in up-regulated DEGs in Nthy/V600E cells with growth factor treatment. Analysis was performed by DAVID.*

Term	Count	%	*p*-Value	Total genes
hsa03010:Ribosome	21	0.207	0.005	87
hsa04210:Apoptosis	14	0.138	0.005	87
hsa00600:Sphingolipid metabolism	8	0.079	0.005	39
hsa05222:Small cell lung cancer	11	0.108	0.015	84
hsa05014:Amyotrophic lateral sclerosis (ALS)	8	0.079	0.024	53
hsa04940:Type I diabetes mellitus	7	0.069	0.025	42
hsa05200:Pathways in cancer	27	0.266	0.032	328
hsa05130:Pathogenic *Escherichia coli* infection	8	0.079	0.035	57
hsa05210:Colorectal cancer	10	0.098	0.038	84
hsa00750:Vitamin B6 metabolism	3	0.03	0.038	6
hsa04110:Cell cycle	13	0.128	0.039	125
hsa04640:Hematopoietic cell lineage	10	0.098	0.043	86
hsa04115:p53 signaling pathway	8	0.079	0.075	68

increase in ERK1/2 activation and cyclin D1 induction (32). In lung cancer and colorectal cancer, *ANO1* overexpression was related to tumor growth and invasion (33, 34).

The *SERPINE2* gene encodes a member of the serpine protein family that inhibits serine proteases. In a study using human colorectal cell lines, *BRAF*^{V600E} increased *SERPINE2* mRNA and protein levels and subsequent MEK/ERK activity (35). In a pancreatic cancer study using nude mouse xenografts, *SERPINE2* overexpression increased invasion through the extracellular matrix. In addition, cancer cells in *SERPINE2*-expressing tumors showed a spindle-shaped morphology and expressed the mesenchymal intermediate filament marker vimentin, which is consistent with our experimental results (36).

SFRP1 is the most extensively characterized gene in the *SFRP* family. This well-established tumor-suppressor gene generally acts as a Wnt inhibitor (37, 38). In expression and functional analysis using glioma stem cells, *SFRP1* regulated the cell cycle and p53 pathways to inhibit Wnt (39). *SFRP1* also increased ERK activity in lung epithelial cell lines (40).

Although Nthy is an immortalized cell line and may incompletely represent characteristics of normal human thyroid cells *in vivo*, our Nthy/V600E cells showed distinctive *BRAF*^{V600E} mutation-associated features compared with Nthy/Vector cells. Nthy/V600E cells show a spindle-shaped morphology, anchorage-independent growth, increased invasive potential, and increased ERK phosphorylation. This cellular behavior was supported by GO analysis (cell adhesion, migration, and proliferation) of microarrays. Genes overexpressed in Nthy/V600E cells were also associated with ERK1/2, the MAPK cascade, and cancer-related pathways. Even if the results of this study cannot fully explain the pathogenesis of thyroid cancer, these Nthy/BRAF cells may be useful for basic research to evaluate the effect of the *BRAF*^{V600E} mutation in normal human thyroid cells.

In conclusion, we generated a new cell line model aiming to study the carcinogenic mechanism of the *BRAF*^{V600E} mutation. Functional experiments and microarrays revealed that Nthy/V600E cells have increased growth and invasion potential and increased expression of MAPK pathway components. Our Nthy/WT and Nthy/BRAF cell lines model human *BRAF*^{V600E} PTC and may be useful in revealing the molecular characteristics of *BRAF*-mutant thyroid cancer.

Conflicts of Interest

None.

Acknowledgements

This study was supported by grants from Seoul National University Hospital (nos. 03-2012-0420, 04-2012-1050, and 30-2012-0070). Handling of lentivirus and genetically modified cells were performed in biosafety level 2 facilities with a permission from the Ministry of Science, ICT and Future Planning of Korea (Permit number: LML08-986).

References

1 Nucera C, Goldfarb M, Hodin R and Parangi S: Role of B-Raf(V600E) in differentiated thyroid cancer and preclinical validation of compounds against B-Raf(V600E). Biochim Biophys Acta *1795(2)*: 152-161, 2009.

2 Garnett MJ, Marais R: Guilty as charged: B-RAF is a human oncogene. Cancer Cell *6(4)*: 313-319, 2004.

3 Carta C, Moretti S, Passeri L, Barbi F, Avenia N, Cavaliere A, Monacelli M, Macchiarulo A, Santeusanio F, Tartaglia M and Puxeddu E: Genotyping of an Italian papillary thyroid carcinoma cohort revealed high prevalence of BRAF mutations, absence of RAS mutations and allowed the detection of a new mutation of BRAF oncoprotein (BRAF(V599lns)). Clin Endocrinol *64(1)*: 105-109, 2006.

4 Kim TY, Kim WB, Song JY, Rhee YS, Gong G, Cho YM, Kim SY, Kim SC, Hong SJ and Shong YK: The BRAF mutation is not associated with poor prognostic factors in Korean patients with conventional papillary thyroid microcarcinoma. Clin Endocrinol *63(5)*: 588-593, 2009.

5 Ahn D, Park JS, Sohn JH, Kim JH, Park S-K, Seo AN and Park JY: *BRAF*^{V600E} mutation does not serve as a prognostic factor in Korean patients with papillary thyroid carcinoma. Auris Nasus Larynx *39(2)*: 198-203, 2012.

6 Mitsutake N, Knauf JA, Mitsutake S, Mesa C Jr., Zhang L and Fagin JA: Conditional *BRAF*^{V600E} expression induces DNA synthesis, apoptosis, dedifferentiation, and chromosomal instability in thyroid PCCL3 cells. Cancer Res *65(6)*: 2465-2473, 2005.

7 Lemoine NR, Mayall ES, Jones T, Sheer D, McDermid S, Kendall-Taylor P and Wynford-Thomas D: Characterisation of human thyroid epithelial cells immortalised *in vitro* by simian virus 40 DNA transfection. Brit J Cancer *60(6)*: 897-903, 1989.

8 Eisenberg MC, Kim Y, Li R, Ackerman WE, Kniss DA and Friedman A: Mechanistic modeling of the effects of myoferlin on tumor cell invasion. PNAS *108(50)*: 20078-20083, 2011.

9 Team RC: R: A language and environment for statistical computing. R Foundation for Statistical Computing, 2015.

10 Du P, Kibbe WA and Lin SM: 'lumi: a pipeline for processing Illumina microarray'. Bioinformatics *24(13)*: 1547-1548, 2008.

11 Lin SM, Du P and Kibbe WA: Model-based Variance-stabilizing Transformation for Illumina Microarray Data. Nucleic Acids Res *36*: e11, 2008.

12 Ritchie ME, Phipson B, Wu D, Hu Y, Law CW, Shi W and Smyth GK: Limma powers differential expression analyses for RNA-sequencing and microarray studies. Nucleic Acids Res *43(7)*: e47, 2015.

13 Falcon S and Gentleman R: Using GO stats to test gene lists for GO term association. Bioinformatics *23(2)*: 257-258, 2007.

14 Huang DW, Sherman BT, Tan Q, Kir J, Liu D, Bryant D, Guo Y, Stephens R, Baseler MW, Lane HC and Lempicki RA: DAVID Bioinformatics Resources: expanded annotation database and novel algorithms to better extract biology from large gene lists. Nucleic Acids Res *35(Web Server issue)*: W169-75, 2007.

15 Welander J, Andreasson A, Juhlin CC, Wiseman RW, Bäckdahl M, Höög A, Larsson C, Gimm O and Söderkvist P: Rare germline mutations identified by targeted next-generation sequencing of susceptibility genes in pheochromocytoma and paraganglioma. J Clin Endocrinol Metab *99(7)*: E1352-1360, 2014.

16 Sato R, Semba T, Saya H and Arima Y: Concise Review: Stem Cells and Epithelial-Mesenchymal Transition in Cancer: Biological Implications and Therapeutic Targets. Stem Cells *34(8)*: 1997-2007, 2016.

17 Wan PT, Garnett MJ, Roe SM, Lee S, Niculescu-Duvaz D, Good VM, Jones CM, Marshall CJ, Springer CJ, Barford D and Marais R: Mechanism of activation of the RAF-ERK signaling pathway by oncogenic mutations of B-RAF. Cell *116(6)*: 855-867, 2004.

18 Xing J, Liu R, Xing M and Trink B: The BRAF T 1799A mutation confers sensitivity of thyroid cancer cells to the *BRAF*^{V600E} inhibitor PLX4032 (RG7204). Biochem Biophys Res Commun *404(4)*: 958-962, 2011.

19 Yang H, Higgins B, Kolinsky K, Packman K, Go Z, Iyer R, Kolis S, Zhao S, Lee R, Grippo JF, Schostack K, Simcox ME, Heimbrook D, Bollag G and Su F: RG7204 (PLX4032), a selective *BRAF*^{V600E} inhibitor, displays potent antitumor activity in preclinical melanoma models. Cancer Res *70(13)*: 5518-5527, 2010.

20 Melillo RM, Castellone MD, Guarino V, De Falco V, Cirafici AM, Salvatore G, Caiazzo F, Basolo F, Giannini R, Kruhoffer M, Orntoft T, Fusco A and Santoro M: The RET/PTC-RAS-BRAF linear signaling cascade mediates the motile and mitogenic phenotype of thyroid cancer cells. J Clin Invest *115(4)*: 1068-1081, 2005.

21 Melillo RM, Castellone MD, Guarino V, De Falco V, Cirafici AM, Salvatore G, Caiazzo F, Basolo F, Giannini R, Kruhoffer M, Orntoft T, Fusco A and Santoro M: Conditional activation of RET/PTC3 and *BRAF*^{V600E} in thyroid cells is associated with gene expression profiles that predict a preferential role of BRAF in extracellular matrix remodeling. Cancer Res *66(13)*: 6521-6529, 2006.

22 Liu D, Liu Z, Condouris S and Xing M: BRAF V600E maintains proliferation, transformation, and tumorigenicity of BRAF-mutant papillary thyroid cancer cells. J Clin Endocrinol Metab *92(6)*: 2264-2271, 2007.

23 Borthwick LA: The IL-1 cytokine family and its role in inflammation and fibrosis in the lung. Semin Immunopathol *38(4)*: 517, 2016.

24 Apte RN and Voronov E: Interleukin-1--a major pleiotropic cytokine in tumor-host interactions. Semin Cancer Biol *12(4)*: 277-290, 2002.

25 Khalili JS, Liu S, Rodríguez-Cruz TG, Whittington M, Wardell S, Liu C, Zhang M, Cooper ZA, Frederick DT, Li Y, Zhang M, Joseph RW, Bernatchez C, Ekmekcioglu S, Grimm E, Radvanyi LG, Davis RE, Davies MA, Wargo JA, Hwu P and Lizée G: Oncogenic BRAF(V600E) promotes stromal cell-mediated immunosuppression via induction of interleukin-1 in melanoma. Clin Cancer Res *18(19)*: 5329-5340, 2012.

26 Khalili JS, Hwu P and Lizee G: Forging a link between oncogenic signaling and immunosuppression in melanoma. Oncoimmunology *2(2)*: e22745, 2013.

27 Rebuffat SA, Kammoun-Krichen M, Charfeddine I, Ayadi H, Bougacha-Elleuch N and Peraldi-Roux S: IL-1beta and TSH disturb thyroid epithelium integrity in autoimmune thyroid diseases. Immunobiology *218(3)*: 285-291, 2013.

28 Resende C, Regalo G, Duraes C, Pinto MT, Wen X, Figueiredo C, Carneiro F and Machado JC: Interleukin-1B signalling leads to increased survival of gastric carcinoma cells through a CREB-C/EBPbeta-associated mechanism. Gastric cancer *19(1)*: 74-84, 2016.

29 Sun H, Chung WC, Ryu SH, Ju Z, Tran HT, Kim E, Kurie JM and Koo JS: Cyclic AMP-responsive element binding protein- and nuclear factor-kappaB-regulated CXC chemokine gene expression in lung carcinogenesis. Cancer Prev Res (Phila) *1(5)*: 316-328, 2008.

30 Chhabra A, Fernando H, Watkins G, Mansel RE and Jiang WG: Expression of transcription factor CREB1 in human breast cancer and its correlation with prognosis. Oncol Rep *18(4)*: 953-958, 2007.

31 Seo Y, Park J, Kim M, Lee HK, Kim JH, Jeong JH and Namkung W: Inhibition of ANO1/TMEM16A Chloride Channel by Idebenone and Its Cytotoxicity to Cancer Cell Lines. PLoS One *10(7)*: e0133656, 2015.

32 Duvvuri U, Shiwarski DJ, Xiao D, Bertrand C, Huang X, Edinger RS, Rock JR, Harfe BD, Henson BJ, Kunzelmann K, Schreiber R, Seethala RS, Egloff AM, Chen X, Lui VW, Grandis JR and Gollin SM: TMEM16A induces MAPK and contributes directly to tumorigenesis and cancer progression. Cancer Res *72(13)*: 3270-3281, 2012.

33 Jia L, Liu W, Guan L, Lu M and Wang K: Inhibition of Calcium-Activated Chloride Channel ANO1/TMEM16A Suppresses Tumor Growth and Invasion in Human Lung Cancer. PloS one *10(8)*: e0136584, 2015.

34 Sui Y, Sun M, Wu F, Yang L, Di W, Zhang G, Zhong L, Ma Z, Zheng J, Fang X and Ma T: Inhibition of TMEM16A expression suppresses growth and invasion in human colorectal cancer cells. PloS one *9(12)*: e115443, 2014.

35 Bergeron S, Lemieux E, Durand V, Cagnol S, Carrier JC, Lussier JG, Boucher MJ and Rivard N: The serine protease inhibitor serpinE2 is a novel target of ERK signaling involved in human colorectal tumorigenesis. Mol Cancer *9*: 271, 2010.

36 Buchholz M, Biebl A, Neesse A, Wagner M, Iwamura T, Leder G, Adler G and Gress TM: SERPINE2 (protease nexin I) promotes extracellular matrix production and local invasion of pancreatic tumors *in vivo*. Cancer Res *63(16)*: 4945-4951, 2003.

37 Bovolenta P, Esteve P, Ruiz JM, Cisneros E and Lopez-Rios J: Beyond Wnt inhibition: new functions of secreted Frizzled-related proteins in development and disease. J Cell Sci *121(6)*: 737-746, 2008.

38 Rubin JS, Barshishat-Kupper M, Feroze-Merzoug F and Xi ZF: Secreted WNT antagonists as tumor suppressors: pro and con. Front Biosci *11*: 2093-2105, 2006.

39 Kierulf-Vieira KS, Sandberg CJ, Grieg Z, Gunther CC, Langmoen IA and Vik-Mo EO: Wnt inhibition is dysregulated in gliomas and its re-establishment inhibits proliferation and tumor sphere formation. Exp Cell Res *340(1)*: 53-61, 2016.

40 Foronjy R, Imai K, Shiomi T, Mercer B, Sklepkiewicz P, Thankachen J, Bodine P and D'Armiento J: The divergent roles of secreted frizzled related protein-1 (SFRP1) in lung morphogenesis and emphysema. Am J Pathol *177(2)*: 598-607, 2010.

Received October 7, 2016
Revised December 5, 2016
Accepted December 6, 2016